

# Integrated cooperative localization of heterogeneous measurement swarm: A unified data-driven method

Kunrui Ze, Wei Wang, *IEEE Senior Member*, Guibin Sun, Jiaqi Yan, Kexin Liu, Jinhu Lü, *IEEE Fellow*

**Abstract**—The cooperative localization (CL) problem in heterogeneous robotic systems with different measurement capabilities is investigated in this work. In practice, heterogeneous sensors lead to directed and sparse measurement topologies, whereas most existing CL approaches rely on multilateral localization with restrictive multi-neighbor geometric requirements. To overcome this limitation, we enable pairwise relative localization (RL) between neighboring robots using only mutual measurement and odometry information. A unified data-driven adaptive RL estimator is first developed to handle heterogeneous and unidirectional measurements. Based on the convergent RL estimates, a distributed pose-coupling CL strategy is then designed, which guarantees CL under a weakly connected directed measurement topology, representing the least restrictive condition among existing results. The proposed method is independent of specific control tasks and is validated through a formation control application and real-world experiments.

**Index Terms**—Heterogeneous measurement, cooperative localization, adaptive estimation, nonholonomic robots.

## I. INTRODUCTION

To achieve multi-robot cooperation in unstructured environments where external localization systems such as GPS are unavailable, cooperative localization (CL) is a fundamental capability. The CL task aims to enable each robot to estimate its relative pose with respect to a leader or reference robot using only local measurements and distributed interactions with neighboring robots [1], [2]. In practical robotic systems, multiple sensing modalities are often deployed to enhance robustness. However, due to the possibility of environmental interference or physical damage to sensors, such as the failure of bearing sensors in strong light and dark environments, the sensors available for each robot may be different. Such sensing heterogeneity naturally results in sparse and directed measurement topologies. Therefore, it is essential to investigate CL task under heterogeneous measurement conditions.

Existing studies on CL in heterogeneous robot swarm typically impose specific assumptions on the measurement topology to ensure observability and convergence. Representative works include [3], which achieves CL under a multi-layer heterogeneous sensing architecture. Another representative study [4] investigates what inter-robot measurements are sufficient

to ensure network localizability. Despite differences in sensing modalities, most existing approaches follow a multilateral localization paradigm, in which each robot recovers its pose from measurements to multiple neighbors and propagates the estimate across the network. As a result, various structural conditions are imposed on the measurement topology to guarantee sufficient geometric constraints, including localizability requirements [1], [5], specific graph constructions such as Henneberg and twin leader-follower frameworks [6], [7], the minimum number of neighbors and non-degenerate geometric conditions on their relative placement [8], [9], or directed topologies containing a spanning tree [10], [11].

While these multilateral localization mechanisms provide sufficient constraints for pose estimation, they inherently require each robot to access measurements from multiple neighbors, which significantly limits applicability in heterogeneous sensing environments. In practice, relative measurements may be sparse, different, or even unavailable for certain robots due to sensor diversity or failures, rendering such topological conditions difficult to satisfy. Consequently, existing CL methods are generally unable to operate under weakly connected or directed measurement topologies. This exposes a fundamental and largely unexplored challenge: How to achieve reliable relative localization (RL) between arbitrary neighboring robot pairs in a unified manner, without relying on multilateral measurements or restrictive topological assumptions.

Motivated by the above limitations, this paper proposes a unified data-driven CL method for heterogeneous robot swarm. Different from existing approaches that rely on multilateral localization using relative measurements from multiple neighbors, the proposed method achieves RL at the pairwise level between neighboring robots in a data-driven manner, which provides the foundation for the overall CL method. Based on the pairwise RL mechanism, distributed CL estimators are further developed to accomplish CL task under a weakly connected directed measurement graph, which represents one of the least restrictive conditions on the measurement topology compared to existing CL methods. As a result, the proposed method avoids stringent structural requirements such as Henneberg-type constructions and offers improved scalability and practicality. Finally, the effectiveness of the proposed strategy is validated through its application to formation control experiment of three-dimensional nonholonomic robots.

**Notations:** Define  $\mathcal{O}_i$  as the odometer reference frame of robot  $i$ , which is fixed at the initial time  $t_0$ , and  $\Sigma_i$  as the body frame attached to robot  $i$ . At time  $t_0$ , the two frames coincide in both position and orientation. In this work, the relative orientation between coordinate frames only involves a yaw rotation. the rotation matrix between frames  $\mathcal{T}_1$  and  $\mathcal{T}_2$

This work was supported in part by the National Key Research and Development Program of China under Grant 2022YFB3305600, and in part by the National Natural Science Foundation of China under Grants 625B2017, 62503028, 62141604 and 62373019. (*Corresponding authors: Jinhu Lü.*)

Kunrui Ze, Guibin Sun Jiaqi Yan and Kexin Liu are with the School of Automation Science and Electrical Engineering, Beihang University, Beijing 100191, China (e-mail: kr\_ze@buaa.edu.cn; sunguibinx@buaa.edu.cn; jqyan@buaa.edu.cn, kxliu@buaa.edu.cn). Wei Wang and Jinhu Lü are with the School of Automation Science and Electrical Engineering, Beihang University, Beijing 100191, China, and also with the Zhongguancun Laboratory, Beijing 100083, China (e-mail: w.wang@buaa.edu.cn; jhlu@iss.ac.cn).

is parameterized by the relative yaw angle  $\theta_{T_2}^{\mathcal{T}_1}$  and defined as

$$\mathbf{R}_{T_2}^{\mathcal{T}_1} = \begin{bmatrix} \cos \theta_{T_2}^{\mathcal{T}_1} & -\sin \theta_{T_2}^{\mathcal{T}_1} & 0 \\ \sin \theta_{T_2}^{\mathcal{T}_1} & \cos \theta_{T_2}^{\mathcal{T}_1} & 0 \\ 0 & 0 & 1 \end{bmatrix} \triangleq \mathbf{R}(\cos \theta_{T_2}^{\mathcal{T}_1}, \sin \theta_{T_2}^{\mathcal{T}_1}).$$

In the remainder of this paper,  $\mathbf{R}_{T_2}^{\mathcal{T}_1}$  and  $\mathbf{R}(\cos \theta_{T_2}^{\mathcal{T}_1}, \sin \theta_{T_2}^{\mathcal{T}_1})$  are used interchangeably. For ease of reading, we list the main symbols of this paper in Appendix A.

## II. PRELIMINARIES AND PROBLEM FORMULATION

### A. Robot model

Consider  $N + 1$  mobile robots in  $\mathbb{R}^3$  which are modeled as

$$\dot{\mathbf{z}}_i^{\mathcal{O}_i}(t) = \begin{bmatrix} \cos \theta_{\Sigma_i}^{\mathcal{O}_i}(t) & 0 \\ \sin \theta_{\Sigma_i}^{\mathcal{O}_i}(t) & 0 \\ 0 & 1 \end{bmatrix} \mathbf{v}_i^{\mathcal{O}_i}, \quad \dot{\theta}_{\Sigma_i}^{\mathcal{O}_i}(t) = w_i, \quad (1)$$

where  $\mathbf{z}_i^{\mathcal{O}_i}$  and  $\theta_{\Sigma_i}^{\mathcal{O}_i}$  represent the translational and rotational displacement of the robot body frame  $\Sigma_i$  with respect to the initial odometer frame  $\mathcal{O}_i$ , which are measurable from the onboard odometry.  $\mathbf{v}_i^{\mathcal{O}_i} \in \mathbb{R}^2$  and  $w_i$  represent the linear velocity and yaw rate of robot  $i$  in frame  $\mathcal{O}_i$ , respectively.  $v_{\max}$  and  $w_{\max}$  denote the upper bounds of the linear velocity and yaw rate of robot  $i$ , i.e.,  $|w_i| \leq w_{\max}$  and  $\|\mathbf{v}_i^{\mathcal{O}_i}\| \leq v_{\max}$ . In this paper, heterogeneity refers to the differences in perception capabilities of robots. While the kinematic model (1), describing the evolution of position and yaw, is unified for all robots, it serves as a generic abstraction without relying on specific nonholonomic constraints.

### B. Measurement topology and communication topology

To formalize the relative geometry between robots  $i$  and  $j$ , define  $\mathbf{p}_{ij}^{\mathcal{O}_i}(t_0)$  as the initial relative position in frame  $\mathcal{O}_i$  and  $\mathbf{R}_{\mathcal{O}_i}^{\mathcal{O}_j} := \mathbf{R}(\cos \theta_{\mathcal{O}_i}^{\mathcal{O}_j}(t_0), \sin \theta_{\mathcal{O}_i}^{\mathcal{O}_j}(t_0))$  as the rotation matrix from  $\mathcal{O}_i$  to  $\mathcal{O}_j$ , where  $\theta_{\mathcal{O}_i}^{\mathcal{O}_j}(t_0)$  is the initial relative yaw angle between robot  $i$  and  $j$ . Both  $\mathbf{p}_{ij}^{\mathcal{O}_i}(t_0)$  and  $\mathbf{R}_{\mathcal{O}_i}^{\mathcal{O}_j}$  are unknown. With the odometer, the following equations hold:

$$\begin{aligned} \mathbf{p}_{ij}^{\Sigma_i}(t) &= \left(\mathbf{R}_{\Sigma_i}^{\mathcal{O}_i}\right)^T \left(\mathbf{p}_{ij}^{\mathcal{O}_i}(t_0) + \mathbf{z}_i^{\mathcal{O}_i}(t) - \left(\mathbf{R}_{\mathcal{O}_i}^{\mathcal{O}_j}\right)^T \mathbf{z}_j^{\mathcal{O}_j}(t)\right), \\ \mathbf{R}_{\Sigma_i}^{\Sigma_j} &= \left(\mathbf{R}_{\Sigma_j}^{\mathcal{O}_j}\right)^T \mathbf{R}_{\mathcal{O}_i}^{\mathcal{O}_j} \mathbf{R}_{\Sigma_i}^{\mathcal{O}_i}, \end{aligned} \quad (2)$$

where  $\mathbf{p}_{ij}^{\Sigma_i}$  denotes the real-time relative position between robots  $i$  and  $j$  in frame  $\Sigma_i$ .  $\mathbf{z}_i^{\mathcal{O}_i}(t)$  and  $\mathbf{R}_{\Sigma_i}^{\mathcal{O}_i} = \mathbf{R}(\cos \theta_{\Sigma_i}^{\mathcal{O}_i}, \sin \theta_{\Sigma_i}^{\mathcal{O}_i})$  can be measured through odometer by robot  $i$  directly, similar to  $\mathbf{z}_j^{\mathcal{O}_j}(t)$  and  $\mathbf{R}_{\Sigma_j}^{\mathcal{O}_j}$ . In a heterogeneous robot swarm, some robots are equipped with relative sensors, while others rely solely on odometry. Let  $m_{ij}^{\Sigma_i}(t_k)$  denote the measurement obtained by robot  $i$  with respect to robot  $j$  at time  $t_k$  and satisfies

$$m_{ij}^{\Sigma_i}(t_k) \in \{\mathbf{p}_{ij}^{\Sigma_i}, d_{ij} = \|\mathbf{p}_{ij}^{\Sigma_i}\|, \phi_{ij}^{\Sigma_i} = \frac{\mathbf{p}_{ij}^{\Sigma_i}}{\|\mathbf{p}_{ij}^{\Sigma_i}\|}, \emptyset\},$$

where  $\mathbf{p}_{ij}^{\Sigma_i}$ ,  $d_{ij}$ , and  $\phi_{ij}^{\Sigma_i}$  denote the relative position, distance, and bearing of robot  $j$  with respect to robot  $i$ , expressed in frame  $\Sigma_i$  and obtained using relative sensors. The symbol  $\emptyset$

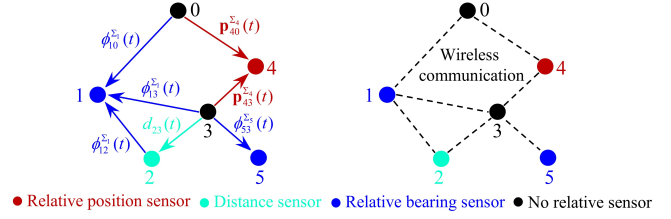


Fig. 1. An example of measurement topology and communication topology. Left: measurement topology. Right: communication topology.

indicates that robot  $i$  is not equipped with any relative sensors and relies solely on odometry (e.g., robot 3 in Fig. 1).

**Measurement topology:** The *directed measurement topology* is described as  $\bar{\mathcal{G}} = (\mathcal{V}, \bar{\mathcal{E}})$ , each node  $\mathcal{V}_i \in \mathcal{V}$  represents a robot. A directed edge  $(i, j) \in \bar{\mathcal{E}}$  from robot  $j$  to robot  $i$  indicates that robot  $i$  can measure one of the following relative quantities with respect to robot  $j$ , i.e.  $m_{ij}^{\Sigma_i}(t_k) \in \{\mathbf{p}_{ij}^{\Sigma_i}, d_{ij}, \phi_{ij}^{\Sigma_i}\}$ . Robots  $i$  and  $j$  are defined as neighboring robots if  $(i, j) \in \bar{\mathcal{E}}$  or  $(j, i) \in \bar{\mathcal{E}}$ .

**Communication topology:** In this paper, neighboring robots are assumed to be able to exchange information through an undirected communication network. This assumption is physically reasonable and widely adopted in CL studies [4], [9], since wireless communication is typically symmetric and less susceptible to environmental interference than directional sensors such as cameras. Accordingly, the *undirected communication topology*  $\mathcal{G} = (\mathcal{V}, \mathcal{E})$  is modeled as  $\bar{\mathcal{G}} = (\mathcal{V}, \bar{\mathcal{E}})$ , where  $(i, j) \in \mathcal{E}$  if and only if  $(i, j) \in \bar{\mathcal{E}}$  or  $(j, i) \in \bar{\mathcal{E}}$ . Let  $\mathcal{L}$  denote the Laplacian matrix of  $\mathcal{G}$ , and  $a_{ij} = a_{ji} = 1$  if and only if robot  $i$  and  $j$  are neighboring robots. An example of the directed measurement topology and its corresponding communication topology is shown in Fig. 1.

Without loss of generality, robot 0 is designated as a leader providing a reference frame. Robot  $i$  is referred to as an *informed robot* if robot 0 is a neighbor of it, and the indicator  $\mu_i$  is defined accordingly. Define the informed matrix  $\mathcal{B} = \text{diag}\{\mu_1, \dots, \mu_N\}$ . To achieve the CL task, we introduce the following assumption

**Assumption 1.** The directed measurement graph  $\bar{\mathcal{G}}$  is weakly connected, i.e., its undirected underlying graph is connected.

Note that Assumption 1 is the least restrictive assumption on the measurement topology, when compared with existing results. If this condition is not met, the swarm will be divided into multiple subgroups. Robots in subgroups that do not contain the leader cannot accomplish CL to the leader. Under Assumption 1, the communication topology is connected.

### C. Objective of cooperative localization

Define the following transformation matrix  $\mathbf{T}_{\Sigma_i}^{\Sigma_0}$  between the robot  $i$ 's body frame  $\Sigma_i$  and the leader robot 0's body frame  $\Sigma_0$ .

$$\mathbf{T}_{\Sigma_i}^{\Sigma_0} := \begin{bmatrix} \mathbf{R}_{\Sigma_i}^{\Sigma_0} & \mathbf{p}_{i0}^{\Sigma_i}(t) \\ \mathbf{0}^T & 1 \end{bmatrix},$$

where  $\mathbf{p}_{i0}^{\Sigma_i}$  denotes the real-time relative position between robot  $i$  and the leader in frame  $\Sigma_i$ .  $\mathbf{R}_{\Sigma_i}^{\Sigma_0}$  is the transformation matrix from frame  $\Sigma_i$  to  $\Sigma_0$ .

For the network robot swarm, the distributed CL task aims to design real-time CL estimator  $\hat{p}_{i0}^{\Sigma_i}$  and  $\hat{R}_{\Sigma_i}^{\Sigma_0}$  to asymptotically estimate  $p_{i0}^{\Sigma_i}$  and  $R_{\Sigma_i}^{\Sigma_0}$  with local relative measurement and communication described by the directed measurement topology and undirected communication topology. Recall (2), the  $z_i^{\mathcal{O}_i}(t)$  and  $R_{\Sigma_i}^{\mathcal{O}_i}$  can be measured through odometer by robot  $i$  directly. To achieve CL task, estimators  $\hat{p}_{i,t_0}$  and  $\hat{R}_{\mathcal{O}_0}^{\mathcal{O}_i}$  should be designed to estimate the initial relative pose  $p_{i0}^{\mathcal{O}_0}(t_0)$  in frame  $\mathcal{O}_0$  and the initial rotation matrix  $R_{\mathcal{O}_i}^{\mathcal{O}_0}$  between robot  $i$  and 0. As a result, the initial relative pose  $p_{ij}^{\mathcal{O}_i}(t_0)$  in frame  $\mathcal{O}_i$  can be estimated as  $(\hat{R}_{\mathcal{O}_i}^{\mathcal{O}_0})^T \hat{p}_{i,t_0}$ . Besides, observer  $\hat{z}_i$  and  $\hat{R}_{\Sigma_0}^{\mathcal{O}_i}$  should be designed to estimate the odometry information  $z_0^{\mathcal{O}_0}(t)$  and  $R_{\Sigma_0}^{\mathcal{O}_0}$  of the leader.

**Remark 1.** *There are two key challenges in performing CL under a heterogeneous measurement topology. First, in a weakly connected measurement graph, a robot may have access to only a single neighbor that is equipped solely with odometry (e.g., robot 5 in Fig. 1), which renders traditional approaches based on multi-neighbor geometric constraints inapplicable. Therefore, achieving RL between arbitrary neighboring robot pairs becomes a critical prerequisite and is addressed in Section III. Second, due to the non-uniform odometer frames of the robots, the coupling between the CL estimation errors of neighboring robots is inherently nonlinear, which prevents the direct application of conventional linear consensus-based methods, such as [12]. Building upon the proposed RL method, the CL problem under non-uniform odometer frames is investigated in Section IV.*

To accomplish the CL task, the following lemma are useful.

**Lemma 1.** [13] *If the undirected graph  $\mathcal{G}$  is connected and at least one robot has direct access to the leader robot 0. The matrix  $(\mathcal{L} + \mathcal{B})$  is positive definite.*

**Lemma 2.** [14] *Consider a perturbed system*

$$\dot{\chi} = f(t, \chi) + g(t, \chi, \Xi), \quad (3)$$

where  $\chi$  is the state and  $\Xi$  is an exogenous signal.  $f(t, \chi)$  and  $g(t, \chi, \Xi)$  are piecewise continuous in  $t$  and locally Lipschitz in  $\chi$  and  $(\chi, \Xi)$ , respectively. Normal system  $\dot{\chi} = f(t, \chi)$  in (3) is uniformly exponentially stable and  $g(t, \chi, \Xi)$  satisfies  $\|g(t, \chi, \Xi)\| \leq a_1 \|\chi\| \|\Xi\| + a_2 \|\Xi\|$ , with two positive constants  $a_1$  and  $a_2$ . Then system (3) uniformly asymptotically stable when  $\|\chi\|$  converges to  $\mathbf{0}$  asymptotically.

### III. RELATIVE LOCALIZATION

Before tackling CL, we first address pairwise RL between arbitrary neighboring robots, which is key to relaxing the measurement-topology dependence of CL. In this section, a unified data-driven adaptive estimator is proposed to achieve RL between neighboring robots.

#### A. Unified relative localization model

Recall (2), since displacements  $z_i^{\mathcal{O}_i}$ ,  $R_{\Sigma_i}^{\mathcal{O}_i}$ ,  $z_j^{\mathcal{O}_j}$  and  $R_{\Sigma_j}^{\mathcal{O}_j}$  are available via odometry and communication. To estimate the real-time relative pose  $p_{ij}^{\Sigma_i}$  and  $R_{\Sigma_i}^{\Sigma_j}$ , the initial relative

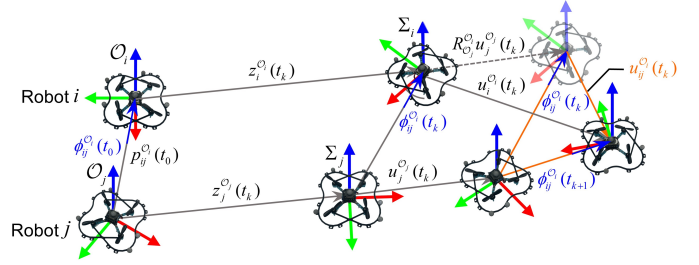


Fig. 2. Geometric relationship between the displacement and unidirectional bearing measurements of the two robots.

position  $p_{ij}^{\mathcal{O}_i}(t_0)$  and initial rotation matrix  $R_{\mathcal{O}_i}^{\mathcal{O}_j}$  from  $\mathcal{O}_i$  to  $\mathcal{O}_j$   $R_{\mathcal{O}_i}^{\mathcal{O}_j}$  should be estimated. In other words, each robot needs to estimate the initial relative state  $\Theta_{ij}^*(t_0) = [p_{ij}^{\mathcal{O}_i}(t_0)^T, \cos \theta_{\mathcal{O}_i}^{\mathcal{O}_j}(t_0), \sin \theta_{\mathcal{O}_i}^{\mathcal{O}_j}(t_0)]$  with the measurements  $m_{ij}^{\Sigma_i}(t_k)$  and  $m_{ji}^{\Sigma_j}(t_k)$  measured in frame  $\Sigma_i$  and  $\Sigma_j$  at time instant  $t_k$ , respectively. where the sampling time instant  $t_k$  is defined as  $t_k \triangleq t_0 + k\Delta t, k \in \mathbb{N}$ . A portion of  $\Theta_{ij}^*(t_0)$  can be directly calculated from the initial relative measurements  $m_{ij}^{\mathcal{O}_i}(t_0)$  and  $m_{ji}^{\mathcal{O}_j}(t_0)$ . The remaining part, denoted as the unknown state  $\Theta_{ij}(t_0)$ , is the key to fully determining the initial relative state. Specifically,  $\Theta_{ij}^*(t_0)$  is uniquely computable if and only if  $\Theta_{ij}(t_0)$  can be estimated. This relationship is governed by the following equation:

$$\Theta_{ij}^*(t_0) = H_{ij}(\Theta_{ij}(t_0), m_{ij}^{\mathcal{O}_i}(t_0), m_{ji}^{\mathcal{O}_j}(t_0)), \quad (4)$$

where  $H_{ij}(\cdot)$  is a known function and is globally Lipschitz continuous to  $\Theta_{ij}(t_0)$ . To estimate the unknown parameter  $\Theta_{ij}(t_0)$ , we aim to construct the following linear observation equation for arbitrary pair of neighboring robots.

$$y_{ij}(t_k) = \Phi_{ij}^{\mathcal{O}_i}(t_k)^T \Theta_{ij}(t_0), \quad (5)$$

where  $y_{ij}(t_k)$  and  $\Phi_{ij}^{\mathcal{O}_i}(t_k)$  are obtainable and can be calculated with the relative sensor and odometer measurement. For neighboring robots equipped with different sensing modalities, the explicit mathematical form of (5) varies accordingly. Details are provided in the next section.

#### B. Observation equation under different sensor combinations

The relative measurements  $m_{ij}^{\Sigma_i}$  and  $m_{ji}^{\Sigma_j}$  between neighboring robots  $i$  and  $j$  may be different. The three configurations in which only one robot has a sensor are a subset of the six configurations in which both robots are equipped; consequently, the measurement data observed in those single-sensor cases are contained within the richer measurement sets of the dual-sensor cases. Therefore, analyzing the observation equations for those three single-sensor cases provides a basis for handling all remaining configurations. Without loss of generality, let robot  $j$  be a sensorless robot, the relative measurement of robot  $i$  for  $j$  at time instant  $t_k$  is  $m_{ij}^{\Sigma_i}(t_k)$ .

**Case 1:**  $m_{ij}^{\Sigma_i} = \phi_{ij}^{\Sigma_i}$  and  $m_{ji}^{\Sigma_j} = \emptyset$

With the initial bearing information  $\phi_{ij}^{\Sigma_i}(t_0)$  obtainable, it can be easily seen that the unknown parameter  $\Theta_{ij}(t_0)$  is  $\Theta_{ij}(t_0) = [d_{ij}(t_0), \cos \theta_{\mathcal{O}_i}^{\mathcal{O}_j}(t_0), \sin \theta_{\mathcal{O}_i}^{\mathcal{O}_j}(t_0)]^T$ . The initial relative state  $\Theta_{ij}^*(t_0)$  can be calculated as  $\Theta_{ij}^*(t_0) =$

$[(\phi_{ij}^{\mathcal{O}_i}(t_0))^\top, \cos \theta_{\mathcal{O}_i}^{\mathcal{O}_j}(t_0), \sin \theta_{\mathcal{O}_i}^{\mathcal{O}_j}(t_0)]^\top$ , which is globally Lipschitz continuous respect to  $\Theta_{ij}(t_0)$ . Next, we construct the observation equation (5) under the single bearing measurement case. Since  $\mathbf{R}_{\mathcal{O}_i}^{\Sigma_i}$  is available,  $\phi_{ij}^{\mathcal{O}_i}(t_k) = (\mathbf{R}_{\mathcal{O}_i}^{\Sigma_i})^\top \phi_{ij}^{\Sigma_i}(t_k)$  is also available and we do not distinguish them below. Define the translational displacement of robot  $i$  from  $t_k$  to  $t_{k+1}$  in its odometer frame  $\mathcal{O}_i$  as  $\mathbf{u}_i^{\mathcal{O}_i}$ , as shown in Fig. 2. Adopt the sine theorem to the orange triangle in Fig. 2, the bearing measured by robot  $i$  from two adjacent samples  $\phi_{ij}^{\mathcal{O}_i}(t_k)$  and  $\phi_{ij}^{\mathcal{O}_i}(t_{k+1})$  satisfy

$$d_{ij}(t_k) \left( \phi_{ij}^{\mathcal{O}_i}(t_k) \times \phi_{ij}^{\mathcal{O}_i}(t_{k+1}) \right) = -\mathbf{u}_i^{\mathcal{O}_i} \times \phi_{ij}^{\mathcal{O}_i}(t_{k+1}), \quad (6)$$

where  $\mathbf{u}_i^{\mathcal{O}_i} = \left( \mathbf{u}_i^{\mathcal{O}_i}(t_k) - (\mathbf{R}_{\mathcal{O}_i}^{\mathcal{O}_j})^\top \mathbf{u}_j^{\mathcal{O}_j}(t_k) \right)$  is the relative translational displacement between robots  $i$  and  $j$  from  $t_k$  to  $t_{k+1}$ . According to (2),  $d_{ij}(t_k)$  satisfies

$$\mathbf{p}_{ij}^{\mathcal{O}_i} = d_{ij}(t_0) \phi_{ij}^{\mathcal{O}_i}(t_0) + \mathbf{z}_i^{\mathcal{O}_i}(t_k) - (\mathbf{R}_{\mathcal{O}_i}^{\mathcal{O}_j})^\top \mathbf{z}_j^{\mathcal{O}_j}(t_k), \quad (7)$$

where  $\mathbf{p}_{ij}^{\mathcal{O}_i} = d_{ij}(t_k) \phi_{ij}^{\mathcal{O}_i}(t_k)$ . Multipling Eq.(6) by vector  $\phi_{ij}^{\mathcal{O}_i}(t_k)$  after converting both sides to rank, it has

$$\begin{aligned} & \mathbf{a}_{ij}(t_k)^\top d_{ij}(t_k) \phi_{ij}^{\mathcal{O}_i}(t_k) + \left( \mathbf{u}_i^{\mathcal{O}_i} \times \phi_{ij}^{\mathcal{O}_i}(t_{k+1}) \right)^\top \phi_{ij}^{\mathcal{O}_i}(t_k) \\ & - \left( \left( (\mathbf{R}_{\mathcal{O}_i}^{\mathcal{O}_j})^\top \mathbf{u}_j^{\mathcal{O}_j}(t_k) \right) \times \phi_{ij}^{\mathcal{O}_i}(t_{k+1}) \right)^\top \phi_{ij}^{\mathcal{O}_i}(t_k) = 0, \end{aligned} \quad (8)$$

where  $\mathbf{a}_{ij}(t_k) \triangleq \left( \phi_{ij}^{\mathcal{O}_i}(t_k) \times \phi_{ij}^{\mathcal{O}_i}(t_{k+1}) \right)$  is measurable. Substituting Eq.(7) to Eq.(8), it has

$$\begin{aligned} & \mathbf{a}_{ij}(t_k)^\top \mathbf{z}_i^{\mathcal{O}_i}(t_k) + \left( \mathbf{u}_i^{\mathcal{O}_i}(t_k) \times \phi_{ij}^{\mathcal{O}_i}(t_{k+1}) \right)^\top \phi_{ij}^{\mathcal{O}_i}(t_k) \\ & = -\mathbf{a}_{ij}(t_k)^\top d_{ij}(t_0) \phi_{ij}^{\mathcal{O}_i}(t_0) + \mathbf{a}_{ij}(t_k)^\top (\mathbf{R}_{\mathcal{O}_i}^{\mathcal{O}_j})^\top \mathbf{z}_j^{\mathcal{O}_j}(t_k) \\ & + \left( \left( (\mathbf{R}_{\mathcal{O}_i}^{\mathcal{O}_j})^\top \mathbf{u}_j^{\mathcal{O}_j}(t_k) \right) \times \phi_{ij}^{\mathcal{O}_i}(t_{k+1}) \right)^\top \phi_{ij}^{\mathcal{O}_i}(t_k). \end{aligned} \quad (9)$$

Define  $\mathbf{a}_{ij} = [a_{ij,1}, a_{ij,2}, a_{ij,3}] \triangleq [\mathbf{a}_{ij,h}^\top, a_{ij,3}]^\top$ . Similarly, take  $\mathbf{z}_j^{\mathcal{O}_j} \triangleq [(\mathbf{z}_{j,h}^{\mathcal{O}_j})^\top, z_{j,3}^{\mathcal{O}_j}]^\top$ ,  $\phi_{ij}^{\mathcal{O}_i} \triangleq [(\phi_{ij,h}^{\mathcal{O}_i})^\top, \phi_{ij,3}^{\mathcal{O}_i}]^\top$  and  $\mathbf{u}_j^{\mathcal{O}_j} \triangleq [(\mathbf{u}_{j,h}^{\mathcal{O}_j})^\top, u_{j,3}^{\mathcal{O}_j}]^\top$ , then one can check that

$$\begin{aligned} & \mathbf{a}_{ij}(t_k)^\top (\mathbf{R}_{\mathcal{O}_i}^{\mathcal{O}_j})^\top \mathbf{z}_j^{\mathcal{O}_j}(t_k) = a_{ij,3}(t_k) z_{j,3}^{\mathcal{O}_j}(t_k) \\ & + [a_{ij,h}(t_k)^\top \mathbf{z}_{j,h}^{\mathcal{O}_j}(t_k), -\mathbf{a}_{ij,h}(t_k)^\top \times \mathbf{z}_{j,h}^{\mathcal{O}_j}(t_k)] \begin{bmatrix} \cos \theta_{\mathcal{O}_i}^{\mathcal{O}_j}(t_0) \\ \sin \theta_{\mathcal{O}_i}^{\mathcal{O}_j}(t_0) \end{bmatrix} \\ & \left( \left( (\mathbf{R}_{\mathcal{O}_i}^{\mathcal{O}_j})^\top \mathbf{u}_j^{\mathcal{O}_j}(t_k) \right) \times \phi_{ij}^{\mathcal{O}_i}(t_{k+1}) \right)^\top \phi_{ij}^{\mathcal{O}_i}(t_k) = -a_{ij,3} u_{j,3}^{\mathcal{O}_j} \\ & + [-\mathbf{u}_{j,h}^{\mathcal{O}_j}(t_k)^\top \mathbf{a}_{ij}(t_k), -\mathbf{u}_{j,h}^{\mathcal{O}_j}(t_k) \times \mathbf{a}_{ij}(t_k)] \begin{bmatrix} \cos \theta_{\mathcal{O}_i}^{\mathcal{O}_j}(t_0) \\ \sin \theta_{\mathcal{O}_i}^{\mathcal{O}_j}(t_0) \end{bmatrix}. \end{aligned} \quad (10)$$

Substituting Eq.(10) to Eq.(9), one can see

$$\begin{aligned} & \bar{y}_{ij}(t_k) \triangleq \left( \mathbf{u}_i^{\mathcal{O}_i}(t_k) \times \phi_{ij}^{\mathcal{O}_i}(t_{k+1}) \right)^\top \phi_{ij}^{\mathcal{O}_i}(t_k) \\ & + \mathbf{a}_{ij}(t_k)^\top \mathbf{z}_i^{\mathcal{O}_i}(t_k) - a_{ij,3}(t_k) z_{j,3}^{\mathcal{O}_j}(t_k) - a_{ij,3} u_{j,3}^{\mathcal{O}_j} \\ & = [\psi_{ij,1}(t_k), \psi_{ij,2}(t_k), \psi_{ij,3}(t_k)]^\top \Theta_{ij}(t_0) \triangleq \Psi_{ij}(t_k)^\top \Theta_{ij}(t_0), \end{aligned} \quad (11)$$

where  $\psi_{ij,1}(t_k) = -\mathbf{a}_{ij}(t_k)^\top \phi_{ij}^{\mathcal{O}_i}(t_0)$ ,  $\psi_{ij,2}(t_k) = \mathbf{a}_{ij,h}(t_k)^\top \mathbf{z}_{j,h}^{\mathcal{O}_j}(t_k) - \mathbf{u}_{j,h}^{\mathcal{O}_j}(t_k)^\top \mathbf{a}_{ij,h}(t_k)$  and  $\psi_{ij,3}(t_k) = -\mathbf{u}_{j,h}^{\mathcal{O}_j}(t_k) \times \mathbf{a}_{ij,h}(t_k) - \mathbf{a}_{ij,h}(t_k)^\top \times \mathbf{z}_{j,h}^{\mathcal{O}_j}(t_k)$ . Note that for vector  $\mathbf{x} \in \mathbb{R}^2$ ,  $\mathbf{y} \in \mathbb{R}^2$ ,  $\mathbf{x} \times \mathbf{y} = x[2]y[1] - x[1]y[2]$ . In Eq.(11), one can see that both  $\bar{y}_{ij}(t_k)$  and  $\Psi_{ij}(t_k)$  are available to robot  $i$  at time instant  $t_k$ . The RL problem between robots  $i$  and  $j$  is transformed into a parameter estimation problem for  $\Theta_{ij}(t_0)$ . Define  $y_{ij}(t_k) \triangleq \frac{\bar{y}_{ij}(t_k)}{\|\Psi_{ij}(t_k)\|}$  and normalizing Eq.(11) as

$$y_{ij}(t_k) = \frac{\Psi_{ij}(t_k)}{\|\Psi_{ij}(t_k)\|} \Theta_{ij}(t_0) \triangleq \Phi_{ij}^{\mathcal{O}_i}(t_k)^\top \Theta_{ij}(t_0), \quad (12)$$

which has the same structure with the unified linear model (5)

**Case 2:**  $m_{ij}^{\Sigma_i} = \mathbf{p}_{ij}^{\Sigma_i}$  and  $m_{ji}^{\Sigma_j} = \emptyset$

Similarly to the bearing case, with the relative position  $\mathbf{p}_{ij}^{\mathcal{O}_i}$  in frame  $\mathcal{O}_i$  available, the unknown parameter that needs to be estimated is  $\Theta_{ij}(t_0) = [\cos \theta_{\mathcal{O}_i}^{\mathcal{O}_j}(t_0), \sin \theta_{\mathcal{O}_i}^{\mathcal{O}_j}(t_0)]^\top$ . The initial relative state  $\Theta_{ij}^*(t_0)$  can be directly represented as  $\Theta_{ij}^*(t_0) = [(\mathbf{p}_{ij}^{\mathcal{O}_i})^\top, \cos \theta_{\mathcal{O}_i}^{\mathcal{O}_j}(t_0), \sin \theta_{\mathcal{O}_i}^{\mathcal{O}_j}(t_0)]^\top$ , which is globally Lipschitz continuous respect to  $\Theta_{ij}(t_0)$ . With  $\mathbf{R}_{\Sigma_i}^{\mathcal{O}_i}$  is available,  $\mathbf{p}_{ij}^{\Sigma_i}(t_k) = (\mathbf{R}_{\Sigma_i}^{\mathcal{O}_i})^\top \mathbf{p}_{ij}^{\mathcal{O}_i}(t_k)$  is also available. One can see the following relationship is established:

$$(\mathbf{R}_{\mathcal{O}_i}^{\mathcal{O}_j})^\top \mathbf{u}_j^{\mathcal{O}_j}(t_k) = \left( \mathbf{p}_{ij}^{\mathcal{O}_i}(t_k) + \mathbf{u}_i^{\mathcal{O}_i}(t_k) - \mathbf{p}_{ij}^{\mathcal{O}_i}(t_{k+1}) \right).$$

Let  $\mathbf{p}_{ij}^{\mathcal{O}_i} \triangleq [(\mathbf{p}_{ij,h}^{\mathcal{O}_i})^\top, p_{ij,3}^{\mathcal{O}_i}]^\top$  and  $\mathbf{u}_j^{\mathcal{O}_j} \triangleq [(\mathbf{u}_{j,h}^{\mathcal{O}_j})^\top, u_{j,3}^{\mathcal{O}_j}]^\top$ . One can check that

$$y_{ij}(t_k) = \frac{\Psi_{ij}(t_k)}{\|\Psi_{ij}(t_k)\|} \Theta_{ij}(t_0) \triangleq \Phi_{ij}^{\mathcal{O}_i}(t_k)^\top \Theta_{ij}(t_0). \quad (13)$$

where  $y_{ij}(t_k) \triangleq \frac{\bar{y}_{ij}(t_k)}{\|\Psi_{ij}(t_k)\|}$ ,  $\Psi_{ij}(t_k) \triangleq [\mathbf{p}_{ij,h}^{\mathcal{O}_i}(t_k)^\top \mathbf{u}_{j,h}^{\mathcal{O}_j}(t_k), \mathbf{p}_{ij,h}^{\mathcal{O}_i}(t_k)^\top \times \mathbf{u}_{j,h}^{\mathcal{O}_j}(t_k)]^\top$  and  $\bar{y}_{ij}(t_k) \triangleq \mathbf{p}_{ij}^{\mathcal{O}_i}(t_k)^\top \left( \mathbf{p}_{ij}^{\mathcal{O}_i}(t_k) + \mathbf{u}_i^{\mathcal{O}_i}(t_k) - \mathbf{p}_{ij}^{\mathcal{O}_i}(t_{k+1}) \right) - p_{ij,3}^{\mathcal{O}_i}(t_k) u_{j,3}^{\mathcal{O}_j}(t_k)$ , which has the same structure with (5)

**Case 3:**  $m_{ij}^{\Sigma_i} = d_{ij}$  and  $m_{ji}^{\Sigma_j} = \emptyset$

Since distance measurement  $d_{ij}$  is a scalar, there is no difference between measurements taken by one neighbor and measurements taken by two neighbors. The unknown parameter  $\Theta_{ij}(t_0)$  that needs to be estimated is equal to the initial relative state  $\Theta_{ij}^*(t_0)$ , i.e.  $\Theta_{ij}^*(t_0) = \Theta_{ij}(t_0)$ , which is globally Lipschitz continuous respect to  $\Theta_{ij}(t_0)$ . In such measurement situations, a linear observation equation (5) can also be constructed based on distance measurement and odometer measurement information. The observation equation for this situation can be found in [15] and is elaborated here.

For the other 6 measurement cases, at least one unified observation equation can be constructed based on the above 3 basic scenarios. In the next section, a data-driven observer is designed to accomplish RL task between neighbors.

### C. Data-driven relative localization

For robot  $i$ , define  $\hat{\Theta}_{ij}$  as an estimation of parameter  $\Theta_{ij}(t_0)$  and  $\tilde{\Theta}_{ij} = \hat{\Theta}_{ij} - \Theta_{ij}(t_0)$  as the estimation error. Define the following innovation  $\nu_{ij}(t_k)$

$$\nu_{ij}(t_k) = \hat{\Theta}_{ij}^\top \Phi_{ij}^{\mathcal{O}_i}(t_k) - y_{ij}(t_k) = \tilde{\Theta}_{ij}^\top \Phi_{ij}^{\mathcal{O}_i}(t_k).$$

Based on the relative localization model built in Eq.(5), design the following adaptive RL estimator  $\hat{\Theta}_{ij}$  to estimate  $\Theta_{ij}(t_0)$

$$\begin{aligned}\hat{\Theta}_{ij}(t) &= \hat{\Theta}_{ij}(t_k), \quad t_k < t < t_{k+1} \\ \hat{\Theta}_{ij}(t_{k+1}) &= \hat{\Theta}_{ij}(t_k) - \zeta \sum_{m=1}^{\zeta} \Phi_{ij}(t_m) \nu_{ij}(t_m) \\ &\quad - \zeta \Phi_{ij}(t_k) \nu_{ij}(t_k),\end{aligned}\quad (14)$$

where  $\zeta$  is designed as  $\zeta = \frac{\lambda_{\min}(\mathcal{S}_{ij})}{(\lambda_{\max}(\mathcal{U}_{ij}(t_k)) + \lambda_{\max}(\mathcal{S}_{ij}))^2}$ , with current data matrix  $\mathcal{U}_{ij}(t_k) = \Phi_{ij}(t_k) \Phi_{ij}(t_k)^T$  and recorded data matrix  $\mathcal{S}_{ij} = \sum_{m=1}^{\zeta} \Phi_{ij}(t_m) \Phi_{ij}(t_m)^T$ . Design the initial relative pose estimator as

$$\hat{\Theta}_{ij}^*(t_k) = H_{ij}(\Theta_{ij}(t_k), m_{ij}^{\mathcal{O}_i}(t_0), m_{ji}^{\mathcal{O}_j}(t_0)). \quad (15)$$

Recall that  $m_{ij}^{\mathcal{O}_i}(t_0)$  and  $m_{ji}^{\mathcal{O}_j}(t_0)$  are initial relative measurement information in frame  $\mathcal{O}_i$  and  $\mathcal{O}_j$ . Define the relative pose estimated error as  $\tilde{\Theta}_{ij}^* = \hat{\Theta}_{ij}^* - \Theta_{ij}^*$ . The convergence of the estimated error  $\tilde{\Theta}_{ij}^*$  can be guaranteed with the following full rank condition on the recorded data matrix  $\mathcal{S}_{ij}$ .

**Assumption 2.** *The recorded data matrix  $\mathcal{S}_{ij}$  is full rank.*

Assumption 2 indicates that the data matrix  $\mathcal{S}_{ij}$  contains sufficient information to accomplish RL task. This is a common assumption in adaptive parameter estimation methods. It should be noted that how to design the motion trajectory  $u_i^{\mathcal{O}_i}$  of each robot  $i$  to make the data matrix  $\mathcal{S}_{ij}$  full rank can be accomplished with the existing parameter identification results such as [1], which is not within the scope of this paper.

**Theorem 1.** *Under Assumption 2, the pose estimation error  $\|\tilde{\Theta}_{ij}^*\|$  converges to 0 exponentially.*

*Proof.* Choose a Lyapunov candidate as  $V_{ij}(t_k) = \tilde{\Theta}_{ij}(t_k)^T \tilde{\Theta}_{ij}(t_k)$ . and  $\Delta V_{ij} = V_{ij}(t_{k+1}) - V_{ij}(t_k)$  satisfies

$$\begin{aligned}\Delta V_{ij} &\leq \zeta^2 (\lambda_{\max}(\mathcal{U}_{ij}(t_k)) + \lambda_{\max}(\mathcal{S}_{ij}))^2 \|\tilde{\Theta}_{ij}(t_k)\|^2 \\ &\quad - 2\zeta \lambda_{\min}(\mathcal{S}_{ij}) \|\tilde{\Theta}_{ij}(t_k)\|^2.\end{aligned}\quad (16)$$

Substituting  $\zeta$  into Eq.(16), one can see  $\Delta V_{ij} \leq \frac{-\lambda_{\min}(\mathcal{S}_{ij})^2}{(\lambda_{\max}(\mathcal{U}_{ij}(t_k)) + \lambda_{\max}(\mathcal{S}_{ij}))^2} \|\tilde{\Theta}_{ij}(t_k)\|^2$ . It can be check that the maximum eigenvalue of matrix  $\mathcal{U}_{ij}(t_k) = u_{ij}(t_k) u_{ij}(t_k)^T \in \mathbb{R}^3$  satisfies  $\lambda_{\max}(\mathcal{U}_{ij}(t_k)) = \Phi_{ij}(t_k)^T \Phi_{ij}(t_k) \leq 1$ , and the RL error  $\tilde{\Theta}_{ij}$  satisfies  $\|\tilde{\Theta}_{ij}(t_k)\| \leq \left( \sqrt{1 - \frac{\lambda_{\min}(\mathcal{S}_{ij})^2}{(1 + \lambda_{\max}(\mathcal{S}_{ij}))^2}} \right)^k \|\tilde{\Theta}_{ij}(t_0)\|$ , which indicates that  $\tilde{\Theta}_{ij}$  is global exponentially stable. Since  $H_{ij}(\cdot)$  is globally Lipschitz continuous respect to  $\tilde{\Theta}_{ij}$ ,  $\tilde{\Theta}_{ij}^*(t_k) = \hat{\Theta}_{ij}^*(t_k) - \Theta_{ij}^*$  is also global exponentially stable.  $\square$

For robot  $i$ , redefine the RL estimator (15) as  $\hat{\Theta}_{ij}^*(t_k) \triangleq [(\hat{p}_{ij,t_0}^{\mathcal{O}_i})^T, \hat{c}_{ij,t_0}, \hat{s}_{ij,t_0}]^T$  and redefine the pose estimation error as  $\tilde{\Theta}_{ij}^*(t_k) \triangleq [(\hat{p}_{ij,t_0}^{\mathcal{O}_i})^T, \tilde{c}_{ij,t_0}, \tilde{s}_{ij,t_0}]^T$ . The initial relative pose can be estimated with  $\hat{R}_{\mathcal{O}_i}^{\mathcal{O}_j} = \mathbf{R}(\hat{c}_{ij,t_0}, \hat{s}_{ij,t_0})$ . For robot  $j$ , define  $\hat{c}_{ji,t_0} = \hat{c}_{ij,t_0}$ ,  $\hat{s}_{ji,t_0} = -\hat{s}_{ij,t_0}$  and  $\hat{p}_{ji,t_0}^{\mathcal{O}_j} = -\hat{R}_{\mathcal{O}_i}^{\mathcal{O}_j} \hat{p}_{ij,t_0}^{\mathcal{O}_i}$ , where  $\hat{R}_{\mathcal{O}_i}^{\mathcal{O}_j} = \mathbf{R}(\hat{c}_{ji,t_0}, \hat{s}_{ji,t_0})$ . Then the RL between robots  $i$  and  $j$  can be achieved.

Other relative measurements (e.g., ratio-of-distance or angle [16]) can be integrated into the observation equation of  $\Theta_{ij}$  via odometer augmentation, yielding a unified method.

**Remark 2.** *Different from existing CL methods [3], [4], which build geometric constraints from relative measurements among multiple neighboring robots, our key idea is to design a data-driven RL estimator (14) for each pair of neighboring robots. Implementing CL based on RL over arbitrary neighboring pairs effectively relaxes the stringent requirements on the measurement topology. Moreover, the data-driven design guarantees exponential convergence of the RL estimator (14). As will be shown in Section IV-B, this exponential RL convergence is precisely what ensures the asymptotic convergence of the CL estimator (17). Therefore, data plays a crucial role in guaranteeing the convergence of the CL estimator.*

#### IV. INTEGRATED COOPERATIVE LOCALIZATION

In this section, we present a distributed CL method based on data-driven RL estimator and demonstrate that, under sufficient data collection, the CL estimator converge asymptotically.

##### A. Cooperative localization estimator

The real-time CL estimators  $\hat{p}_{i0}^{\Sigma_i}$  and  $\hat{R}_{\Sigma_i}^{\Sigma_0}$  are designed as

$$\begin{aligned}\hat{p}_{i0}^{\Sigma_i} &= \left( \mathbf{R}_{\Sigma_i}^{\mathcal{O}_i} \right)^T \left( \left( \hat{R}_{\mathcal{O}_i}^{\mathcal{O}_0} \right)^T \hat{p}_{i,t_0} + z_i^{\mathcal{O}_i} - \left( \hat{R}_{\mathcal{O}_i}^{\mathcal{O}_0} \right)^T \hat{z}_i \right), \\ \hat{R}_{\Sigma_i}^{\Sigma_0} &= \left( \hat{R}_{\Sigma_0}^{\mathcal{O}_0} \right)^T \hat{R}_{\mathcal{O}_i}^{\mathcal{O}_0} \mathbf{R}_{\Sigma_i}^{\mathcal{O}_i},\end{aligned}\quad (17)$$

where  $\mathbf{R}_{\Sigma_i}^{\mathcal{O}_i}$  and  $z_i^{\mathcal{O}_i}$  can be measured by odometer of robot  $i$ .  $\hat{p}_{i,t_0}$  and  $\hat{R}_{\mathcal{O}_i}^{\mathcal{O}_0}$  are the distributed coupled estimators which estimate the unknown initial relative pose between robot  $i$  and the leader.  $\hat{z}_i$  and  $\hat{R}_{\Sigma_0}^{\mathcal{O}_0}$  are distributed observers which estimates the leader's odometry information.

1) *Distributed coupled estimator design:* For robot  $i$ , estimators  $\hat{p}_{i,t_0}$  and  $\hat{R}_{\mathcal{O}_i}^{\mathcal{O}_0} = \mathbf{R}(\hat{c}_{i,t_0}, \hat{s}_{i,t_0})$  are designed as,

$$\begin{aligned}\dot{\hat{p}}_{i,t_0} &= \sum_{j \in \mathcal{N}_i} a_{ij} \left( \hat{p}_{j,t_0} + \hat{R}_{\mathcal{O}_i}^{\mathcal{O}_0} \hat{p}_{ij,t_0}^{\mathcal{O}_i} - \hat{p}_{i,t_0} \right) + \mu_i (\hat{p}_{i0,t_0} - \hat{p}_{i,t_0}) \\ \dot{\hat{c}}_{i,t_0} &= \sum_{j \in \mathcal{N}_i} a_{ij} (\hat{c}_{ij,t_0} \hat{c}_{j,t_0} - \hat{s}_{ij,t_0} \hat{s}_{j,t_0} - \hat{c}_{i,t_0}) + \mu_i (\hat{c}_{i0,t_0} - \hat{c}_{i,t_0}) \\ \dot{\hat{s}}_{i,t_0} &= \sum_{j \in \mathcal{N}_i} a_{ij} (\hat{s}_{ij,t_0} \hat{c}_{j,t_0} + \hat{c}_{ij,t_0} \hat{s}_{j,t_0} - \hat{s}_{i,t_0}) + \mu_i (\hat{s}_{i0,t_0} - \hat{s}_{i,t_0}),\end{aligned}\quad (18)$$

where  $\hat{p}_{ij,t_0}^{\mathcal{O}_i}$ ,  $\hat{c}_{ij,t_0}$  and  $\hat{s}_{ij,t_0}$  are the RL estimator defined in the last section.  $\mathcal{N}_i$  is the neighbor set of robot  $i$ .

2) *Distributed observer design:* For robot  $i$  the distributed observer  $\hat{z}_i$  and  $\hat{R}_{\Sigma_0}^{\mathcal{O}_0} = \mathbf{R}(\hat{c}_i, \hat{s}_i)$  are designed as

$$\begin{aligned}\dot{\hat{z}}_i(t) &= -k_1 e_{i,z} - \frac{e_{i,z}^T}{\sqrt{e_{i,z}^T e_{i,z} + \delta}} \hat{F}_{i,z}, \\ \dot{\hat{F}}_{i,z} &= \sum_{j \in \mathcal{N}_i} a_{ij} \left( \hat{F}_{i,z} - \hat{F}_{j,z} \right) + \mu_i \left( \hat{F}_{i,z} - F_z \right), \\ \dot{\hat{c}}_i(t) &= -k_1 e_{i,c} - \frac{e_{i,c}}{\sqrt{e_{i,c}^2 + \delta}}, \quad \dot{\hat{s}}_i(t) = -k_1 e_{i,s} - \frac{e_{i,s}}{\sqrt{e_{i,s}^2 + \delta}},\end{aligned}\quad (19)$$

where  $e_{i,z} = \sum_{j \in \mathcal{N}_i} a_{ij} (\hat{z}_i - \hat{z}_j) + \mu_i (\hat{z}_i - z_0^{\mathcal{O}_0})$ ,  $e_{i,c} = \sum_{j \in \mathcal{N}_i} a_{ij} (\hat{c}_i - \hat{c}_j) + \mu_i (\hat{c}_i - \cos \theta_{\Sigma_0^{\mathcal{O}_0}})$  and  $e_{i,s} = \sum_{j \in \mathcal{N}_i} a_{ij} (\hat{s}_i - \hat{s}_j) + \mu_i (\hat{s}_i - \sin \theta_{\Sigma_0^{\mathcal{O}_0}})$  are the consensus error.  $F_z = v_{\max}$  is the upbound of the first-order derivative of  $z_0^{\mathcal{O}_0}$  and  $\delta = \beta e^{-\alpha t}$ ,  $\beta, \alpha > 0$ . To better illustrate the calculation process of algorithm, we have added pseudocode for the proposed method in Appendix B.

**Remark 3.** Different from the existing research results that rely on hierarchical multi-layer graph [3], Henneberg construction [6] or other assumptions on the measurement topology [4], [10] to ensure that each robot can obtain sufficient measurements from its multiple neighbors, our method accomplish CL task under only weakly connected measurement topology condition, which is also the least restrictive topological condition for CL task. The main reason is that RL estimator (14) and (15) are adopted in the CL estimator (17) and we do not need the measurements from multiple neighbors. Therefore, there are no specific requirements like number, physical position on the neighboring set of each robot.

### B. Convergence analysis

Redefine  $\hat{\mathbf{R}}_{\Sigma_i}^{\Sigma_0} = \mathbf{R} \left( \cos \theta_{\Sigma_i}^{\Sigma_0}, \sin \theta_{\Sigma_i}^{\Sigma_0} \right)$  and define the close-loop real-time estimation error as  $\tilde{\mathbf{p}}_{i0} = \hat{\mathbf{p}}_{i0}^{\Sigma_i} - \mathbf{p}_{i0}^{\Sigma_i}$ ,  $\tilde{\mathbf{c}}_{i0} = \hat{\mathbf{c}}_{i0}^{\Sigma_i} - \mathbf{c}_{i0}^{\Sigma_i}$ ,  $\tilde{\mathbf{s}}_{i0} = \hat{\mathbf{s}}_{i0}^{\Sigma_i} - \mathbf{s}_{i0}^{\Sigma_i}$ . Next, we establish the asymptotic convergence of the coupled estimators (i.e.  $\hat{\mathbf{p}}_{i,t_0}$  and  $\hat{\mathbf{R}}_{\mathcal{O}_i}^{\mathcal{O}_0}$ ) and the distributed observers (i.e.  $\hat{z}_i$  and  $\hat{\mathbf{R}}_{\Sigma_0}^{\mathcal{O}_0}$ ), and subsequently prove the convergence of the real-time CL estimators (i.e.  $\hat{\mathbf{p}}_{i0}^{\Sigma_i}$  and  $\hat{\mathbf{R}}_{\Sigma_i}^{\Sigma_0}$ ).

1) *Convergence of the distributed coupled estimator:* In this section, we establish the asymptotic convergence of the distributed coupled estimators  $\hat{\mathbf{p}}_{i,t_0}(t)$ ,  $\hat{\mathbf{c}}_{i,t_0}(t)$ , and  $\hat{\mathbf{s}}_{i,t_0}(t)$ . To facilitate the convergence analysis, the following definition and lemma are introduced.

**Definition 1.** Define the initial relative yaw angle between robots  $i$  and  $j$  as  $\theta_{\mathcal{O}_i}^{\mathcal{O}_j}$ , take the attitude Laplacian matrix as

$$\mathcal{L}_{\bar{\mathbf{R}}} = \begin{bmatrix} |\mathcal{N}_1| \mathbf{I}_{2 \times 2} & \cdots & -a_{1i} \bar{\mathbf{R}}_{\mathcal{O}_1}^{\mathcal{O}_i} & \cdots & -a_{1N} \bar{\mathbf{R}}_{\mathcal{O}_1}^{\mathcal{O}_N} \\ \vdots & \ddots & \vdots & \ddots & \vdots \\ -a_{i1} \bar{\mathbf{R}}_{\mathcal{O}_i}^{\mathcal{O}_1} & \cdots & |\mathcal{N}_i| \mathbf{I}_{2 \times 2} & \cdots & -a_{iN} \bar{\mathbf{R}}_{\mathcal{O}_i}^{\mathcal{O}_N} \\ \vdots & \ddots & \vdots & \ddots & \vdots \\ -a_{N1} \bar{\mathbf{R}}_{\mathcal{O}_N}^{\mathcal{O}_1} & \cdots & -a_{Ni} \bar{\mathbf{R}}_{\mathcal{O}_N}^{\mathcal{O}_i} & \cdots & |\mathcal{N}_N| \mathbf{I}_{2 \times 2} \end{bmatrix},$$

where  $\bar{\mathbf{R}}_{\mathcal{O}_i}^{\mathcal{O}_j}$  is defined as  $\bar{\mathbf{R}}_{\mathcal{O}_i}^{\mathcal{O}_j} = \begin{bmatrix} \cos \theta_{\mathcal{O}_i}^{\mathcal{O}_j} & -\sin \theta_{\mathcal{O}_i}^{\mathcal{O}_j} \\ \sin \theta_{\mathcal{O}_i}^{\mathcal{O}_j} & \cos \theta_{\mathcal{O}_i}^{\mathcal{O}_j} \end{bmatrix}$ .

**Lemma 3.** If the augmented sensing topology  $\mathcal{G} = (\mathcal{V}, \mathcal{E})$  is connected and at least one of the robot  $i$  is informed, i.e.  $\exists i, \mu_i = 1$ , the coupled information matrix  $(\mathcal{L}_{\bar{\mathbf{R}}} + \mathcal{B} \otimes \mathbf{I}_{2 \times 2})$  is positive definite, i.e.  $(\mathcal{L}_{\bar{\mathbf{R}}} + \mathcal{B} \otimes \mathbf{I}_{2 \times 2}) > 0$ .

*Proof.* To prove  $(\mathcal{L}_{\bar{\mathbf{R}}} + \mathcal{B} \otimes \mathbf{I}_{2 \times 2}) > 0$ , we firstly prove that  $\forall \mathbf{x} \in \mathbb{R}^{2N}$ , inequality  $\mathbf{x}^T (\mathcal{L}_{\bar{\mathbf{R}}} + \mathcal{B} \otimes \mathbf{I}_{2 \times 2}) \mathbf{x} \geq 0$  is hold, then we show that the equal sign only holds when  $\mathbf{x} = \mathbf{0}$ .

Let  $\mathbf{x} = [x_{11}, x_{12}, \dots, x_{N1}, x_{N2}]^T = [\mathbf{x}_1^T, \dots, \mathbf{x}_N^T]^T$ , then  $\mathbf{x}^T (\mathcal{L}_{\bar{\mathbf{R}}} + \mathcal{B} \otimes \mathbf{I}_{2 \times 2}) \mathbf{x}$  can be represented as

$$\begin{aligned} & \mathbf{x}^T (\mathcal{L}_{\bar{\mathbf{R}}} + \mathcal{B} \otimes \mathbf{I}_{2 \times 2}) \mathbf{x} \\ &= \sum_{i=1}^N \sum_{j=1}^N -a_{ij} \mathbf{x}_i^T \bar{\mathbf{R}}_{\mathcal{O}_i}^{\mathcal{O}_j} \mathbf{x}_j + \sum_i |\mathcal{N}_i| \mathbf{x}_i^T \mathbf{x}_i + \sum_i \mu_i \mathbf{x}_i^T \mathbf{x}_i \\ &= \frac{1}{2} \sum_{(i,j) \in \mathcal{E}} \left( -2 \mathbf{x}_i^T \bar{\mathbf{R}}_{\mathcal{O}_i}^{\mathcal{O}_j} \mathbf{x}_j + \mathbf{x}_i^T \mathbf{x}_i + \mathbf{x}_j^T \mathbf{x}_j \right) + \sum_i \mu_i \mathbf{x}_i^T \mathbf{x}_i \\ &= \frac{1}{2} \sum_{(i,j) \in \mathcal{E}} \mathbf{x}_i^T \mathbf{x}_i + \mathbf{x}_j^T \bar{\mathbf{R}}_{\mathcal{O}_j}^{\mathcal{O}_i} \bar{\mathbf{R}}_{\mathcal{O}_i}^{\mathcal{O}_j} \mathbf{x}_j - 2 \mathbf{x}_i^T \bar{\mathbf{R}}_{\mathcal{O}_i}^{\mathcal{O}_j} \mathbf{x}_i + \sum_i \mu_i \mathbf{x}_i^T \mathbf{x}_i \\ &= \frac{1}{2} \sum_{(i,j) \in \mathcal{E}} \left( \mathbf{x}_i - \bar{\mathbf{R}}_{\mathcal{O}_i}^{\mathcal{O}_j} \mathbf{x}_j \right)^T \left( \mathbf{x}_i - \bar{\mathbf{R}}_{\mathcal{O}_i}^{\mathcal{O}_j} \mathbf{x}_j \right) + \sum_i \mu_i \mathbf{x}_i^T \mathbf{x}_i \geq 0. \end{aligned} \quad (20)$$

Note that the second equation is due to the fact that  $\mathbf{x}_i^T \bar{\mathbf{R}}_{\mathcal{O}_i}^{\mathcal{O}_j} \mathbf{x}_j = \left( \mathbf{x}_i^T \bar{\mathbf{R}}_{\mathcal{O}_i}^{\mathcal{O}_j} \mathbf{x}_j \right)^T = \mathbf{x}_j^T \bar{\mathbf{R}}_{\mathcal{O}_j}^{\mathcal{O}_i} \mathbf{x}_i$ . Next, we analyze the situation when the equal sign holds. According to Eq.(20), when the equal sign holds,  $\mathbf{x}_i = \mathbf{0}$ . Due to the reversibility of the rotation matrix  $\bar{\mathbf{R}}_{\mathcal{O}_i}^{\mathcal{O}_j}$ , one can conclude that  $\mathbf{x}_j = \mathbf{0}, \forall a_{ij} = 1$ . Similarly, for each  $j$  in node  $i$ 's neighbor set  $\mathcal{N}_i$ , when the equal sign holds, one can also conclude that  $\mathbf{x}_k = \mathbf{0}, \forall a_{kj} = 1$ . For a connected graph composed of a finite number of nodes, iterate this way and we can prove that  $\mathbf{x}_i = \mathbf{0}, \forall i \in \mathcal{V}$ , i.e.  $\mathbf{x} = \mathbf{0}$ . As a result, the coupled information matrix  $(\mathcal{L}_{\bar{\mathbf{R}}} + \mathcal{B} \otimes \mathbf{I}_{2 \times 2})$  is positive definite.  $\square$

Define the estimation error of the distributed coupled observers  $\hat{\mathbf{p}}_{i,t_0}(t)$ ,  $\hat{\mathbf{c}}_{i,t_0}(t)$  and  $\hat{\mathbf{s}}_{i,t_0}(t)$  as  $\tilde{\mathbf{p}}_{i,t_0}(t) = \hat{\mathbf{p}}_{i,t_0}(t) - \mathbf{p}_{i0}^{\mathcal{O}_i}(t_0)$ ,  $\tilde{\mathbf{c}}_{i,t_0}(t) = \hat{\mathbf{c}}_{i,t_0}(t) - \mathbf{c}_{i,t_0}^{\mathcal{O}_i}(t_0)$  and  $\tilde{\mathbf{s}}_{i,t_0}(t) = \hat{\mathbf{s}}_{i,t_0}(t) - \mathbf{s}_{i,t_0}^{\mathcal{O}_i}(t_0)$ . Define the orientation estimation errors as  $\tilde{\chi}_{t_0} = [\tilde{c}_{1,t_0}, \tilde{s}_{1,t_0}, \dots, \tilde{c}_{N,t_0}, \tilde{s}_{N,t_0}]^T$  and position estimation error as  $\tilde{\mathbf{p}}_{t_0} = [\tilde{\mathbf{p}}_{1,t_0}^T, \dots, \tilde{\mathbf{p}}_{N,t_0}^T]^T$ . The convergence of the CL estimator (18) can be described in the following Theorem 2.

**Theorem 2.** Consider the coupled distributed observer (18), if for each pair of  $(i, j) \in \mathcal{E}$ , Assumption 2 is satisfied, then the estimation error  $\tilde{\mathbf{p}}_{t_0}$  and  $\tilde{\chi}_{t_0}$  converge to  $\mathbf{0}$  asymptotically.

*Proof.* Firstly, we show the asymptotic convergence of the orientation observer  $\hat{\mathbf{c}}_{i,t_0}(t)$  and  $\hat{\mathbf{s}}_{i,t_0}(t)$ . Considering the distributed coupled observer (18), the derivative of  $\tilde{\mathbf{c}}_{i,t_0}(t)$  and  $\tilde{\mathbf{s}}_{i,t_0}(t)$  can be represented as

$$\begin{aligned} \dot{\tilde{\mathbf{c}}}_{i,t_0} &= \sum_{j \in \mathcal{N}_i} a_{ij} \left( \cos \theta_{\mathcal{O}_i}^{\mathcal{O}_j} \tilde{c}_{j,t_0} - \sin \theta_{\mathcal{O}_i}^{\mathcal{O}_j} \tilde{s}_{j,t_0} - \tilde{c}_{i,t_0} \right) - \mu_i \tilde{c}_{i,t_0} \\ &\quad + \sum_{j \in \mathcal{N}_i} a_{ij} \left( \tilde{c}_{ij,t_0} \tilde{c}_{j,t_0} - \tilde{s}_{ij,t_0} \tilde{s}_{j,t_0} \right) + \mu_i \tilde{c}_{i0,t_0}, \\ \dot{\tilde{\mathbf{s}}}_{i,t_0} &= \sum_{j \in \mathcal{N}_i} a_{ij} \left( \sin \theta_{\mathcal{O}_i}^{\mathcal{O}_j} \tilde{c}_{j,t_0} + \cos \theta_{\mathcal{O}_i}^{\mathcal{O}_j} \tilde{s}_{j,t_0} - \tilde{s}_{i,t_0} \right) - \mu_i \tilde{s}_{i,t_0} \\ &\quad + \sum_{j \in \mathcal{N}_i} a_{ij} \left( \tilde{s}_{ij,t_0} \tilde{c}_{j,t_0} + \tilde{c}_{ij,t_0} \tilde{s}_{j,t_0} \right) + \mu_i \tilde{s}_{i0,t_0}. \end{aligned}$$

Take the derivative of  $\tilde{\chi}_{t_0}$  and one can see that the following inequality holds:

$$\dot{\tilde{\chi}}_{t_0} \leq -(\mathcal{L}_{\bar{\mathbf{R}}} + \mathcal{B} \otimes \mathbf{I}_{2 \times 2}) \tilde{\chi}_{t_0} + \|\mathbf{E}_a\| \|\tilde{\chi}_{t_0}\| + \|\mathbf{E}_a\|,$$

where  $\Xi_a \in \mathbb{R}^{2N}$  is defined as

$$\Xi_a = \left[ \sum_{j \in \mathcal{N}_1} |\tilde{c}_{1j,t_0}|, \sum_{j \in \mathcal{N}_1} |\tilde{s}_{1j,t_0}|, \dots, \sum_{j \in \mathcal{N}_N} |\tilde{c}_{Nj,t_0}|, \sum_{j \in \mathcal{N}_N} |\tilde{s}_{Nj,t_0}| \right]^T$$

According to Theorem 1,  $\Xi_a \in \mathbb{R}^{2N}$  converges to  $\mathbf{0}$  exponentially as  $t \rightarrow \infty$ . According to Lemma 3, system  $\dot{\tilde{\chi}}_{t_0} \leq -(\mathcal{L}_{\tilde{R}} + \mathcal{B} \otimes \mathbf{I}_{2 \times 2}) \tilde{\chi}_{t_0}$  is uniformly exponentially stable. According to Lemma 2,  $\tilde{\chi}_{t_0}$  converges to  $\mathbf{0}$  asymptotically. Then we show the convergence of position estimation observer  $\hat{\mathbf{p}}_{i,t_0}(t)$ . Considering the distributed coupled observer (18), the derivative of  $\tilde{\mathbf{p}}_{i,t_0}(t)$  can be represented as

$$\begin{aligned} \dot{\tilde{\mathbf{p}}}_{i,t_0}(t) &= \sum_{j \in \mathcal{N}_i} a_{ij} (\tilde{\mathbf{p}}_{j,t_0} - \tilde{\mathbf{p}}_{i,t_0}) - \mu_i \tilde{\mathbf{p}}_{i,t_0} \\ &+ \sum_{j \in \mathcal{N}_i} a_{ij} \left( \tilde{\mathbf{R}}_{\mathcal{O}_i}^{\mathcal{O}_0} \hat{\mathbf{p}}_{ij,t_0} + \mathbf{R}_{\mathcal{O}_i}^{\mathcal{O}_0} \tilde{\mathbf{p}}_{ij,t_0} \right) + \mu_i \tilde{\mathbf{p}}_{i0,t_0}. \end{aligned}$$

Then the derivative of  $\tilde{\mathbf{p}}_{t_0}$  can be calculated as

$$\dot{\tilde{\mathbf{p}}}_{t_0} = -((\mathcal{L} + \mathcal{B}) \otimes \mathbf{I}_{3 \times 3}) \tilde{\mathbf{p}}_{t_0} + \Xi_p,$$

where  $\Xi_p$  is defined as  $\Xi_p = [\Xi_{1,p}, \dots, \Xi_{N,p}]^T$ , with  $\Xi_{i,p} = \sum_{j \in \mathcal{N}_i} a_{ij} \left( \tilde{\mathbf{R}}_{\mathcal{O}_i}^{\mathcal{O}_0} \hat{\mathbf{p}}_{ij,t_0} + \mathbf{R}_{\mathcal{O}_i}^{\mathcal{O}_0} \tilde{\mathbf{p}}_{ij,t_0} \right) + \mu_i \tilde{\mathbf{p}}_{i0,t_0}$ . According to Lemma 1, system  $\dot{\tilde{\mathbf{p}}}_{t_0} = ((\mathcal{L} + \mathcal{B}) \otimes \mathbf{I}_{3 \times 3}) \tilde{\mathbf{p}}_{t_0}$  is uniformly exponentially stable. According to Theorem 1,  $\Xi_p \in \mathbb{R}^{3N}$  converges to  $\mathbf{0}$  exponentially as  $t \rightarrow \infty$ . According to Lemma 2, we can conclude that  $\tilde{\mathbf{p}}_{t_0}$  converges to  $\mathbf{0}$  asymptotically.

2) *Convergence of the CL estimator:* In this section, we establish the convergence of the real-time CL estimators. Define the observer errors as  $\tilde{\mathbf{z}}_i(t)$ ,  $\tilde{c}_i(t)$  and  $\tilde{s}_i(t)$  as  $\tilde{\mathbf{z}}_i = \hat{\mathbf{z}}_i - \mathbf{z}_i^{\mathcal{O}_0}(t)$ ,  $\tilde{c}_i(t) = \hat{c}_i(t) - \cos \theta_{\Sigma_i}^{\mathcal{O}_0}(t)$  and  $\tilde{s}_i(t) = \hat{s}_i(t) - \sin \theta_{\Sigma_i}^{\mathcal{O}_0}(t)$ . The following theorem establishes the convergence of both the observer errors (i.e.  $\tilde{\mathbf{z}}_i(t)$ ,  $\tilde{c}_i(t)$  and  $\tilde{s}_i(t)$ ) and real-time CL estimation errors (i.e.  $\tilde{\mathbf{p}}_{i0}$ ,  $\cos \theta_{\Sigma_i}^{\mathcal{O}_0}$  and  $\sin \theta_{\Sigma_i}^{\mathcal{O}_0}$ ).

**Theorem 3.** Consider the CL estimator (17) composed of the distributed coupled estimator (18) and distributed observer (19), under Assumptions 1 and 2, the CL estimation error  $\|\tilde{\mathbf{p}}_{i0}\|$ ,  $\cos \theta_{\Sigma_i}^{\mathcal{O}_0}$  and  $\sin \theta_{\Sigma_i}^{\mathcal{O}_0}$  converge to 0 asymptotically.

*Proof.* According to Theorem 2, the coupled estimation error  $\|\tilde{\mathbf{p}}_{i,t_0}(t)\|$ ,  $\tilde{c}_{i,t_0}(t)$ ,  $\tilde{s}_{i,t_0}(t)$  converge to 0 asymptotically. Assumption 1 indicates the undirected communication topology is connected. According to Theorem 1 in [17], the distributed observer error  $\|\tilde{\mathbf{z}}_i\|$ ,  $\tilde{c}_i(t)$  and  $\tilde{s}_i(t)$  converge to 0 asymptotically under the connected communication topology. According to Eq.(17), the close-loop estimator is global Lipschitz to the distributed couple estimator  $\hat{\mathbf{p}}_{i,t_0}$ ,  $\hat{c}_{i,t_0}$  and  $\hat{s}_{i,t_0}$  and the distributed observer  $\hat{\mathbf{z}}_i(t)$ ,  $\hat{c}_i(t)$  and  $\hat{s}_i(t)$ . As a result, the close-loop estimation errors as  $\tilde{\mathbf{p}}_{i0}$ ,  $\cos \theta_{\Sigma_i}^{\mathcal{O}_0}$  and  $\sin \theta_{\Sigma_i}^{\mathcal{O}_0}$  converge to 0 asymptotically if and only if the coupled estimation error  $\hat{\mathbf{p}}_{i,t_0}(t)$ ,  $\hat{c}_{i,t_0}(t)$ ,  $\hat{s}_{i,t_0}(t)$  and the observer error  $\hat{\mathbf{z}}_i(t)$ ,  $\hat{c}_i(t)$  and  $\hat{s}_i(t)$  converge to 0 asymptotically.

## V. APPLICATION AND REAL-WORLD EXPERIMENTS

### A. Application in formation control

We take the distributed formation control of nonholonomic robots as an example to illustrate how our CL method is applied to practical problems.

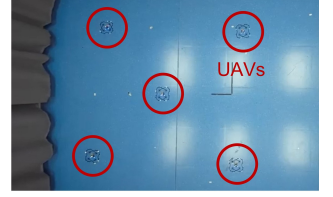
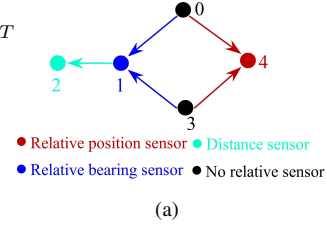


Fig. 3. Experiment setup. (a) Measurement topology. (b) Experimental scene.

Define the desired relative position between robot  $i$  and leader 0 in frame  $\mathcal{O}_0$  as  $\rho_i^{\mathcal{O}_0}$ , assume the acceleration and rotational acceleration of leader is bounded, i.e.  $\|\dot{\mathbf{v}}_0^{\mathcal{O}_0}\| \leq a_{\max}$ ,  $\dot{w}_0 \leq \alpha_{\max}$ . Define the transformed formation error in frame  $\Sigma_i$  as  $\epsilon_i = [\epsilon_{i,p}^T, \epsilon_{i,c}, \epsilon_{i,s}]^T$ , where  $\epsilon_{i,p} = \mathbf{p}_{i0}^{\Sigma_i} - \mathbf{R}_{\mathcal{O}_0}^{\Sigma_i} \rho_i^{\mathcal{O}_0}$ ,  $\epsilon_{i,c} = 1 - \cos \theta_{\Sigma_i}^{\mathcal{O}_0}$  and  $\epsilon_{i,s} = \sin \theta_{\Sigma_i}^{\mathcal{O}_0}$ . Define estimated formation error  $\hat{\epsilon}_i = [\hat{\epsilon}_{i,p}^T, \hat{\epsilon}_{i,c}, \hat{\epsilon}_{i,s}]^T$ , where  $\hat{\epsilon}_{i,p} = \hat{\mathbf{p}}_{i0}^{\Sigma_i} + \mathbf{R}_{\mathcal{O}_i}^{\Sigma_i} \left( \hat{\mathbf{R}}_{\mathcal{O}_i}^{\mathcal{O}_0} \right)^T \rho_i^{\mathcal{O}_0}$ ,  $\hat{\epsilon}_{i,s} = \widehat{\sin \theta_{\Sigma_i}^{\mathcal{O}_0}}$  and  $\hat{\epsilon}_{i,c} = 1 - \widehat{\cos \theta_{\Sigma_i}^{\mathcal{O}_0}}$ . To satisfy Assumption 2, the control strategy consists of two stages including data collection stage and CL estimator convergence stage. In the first control stage, each robot performs data collection according to the preset control program. The control input can be designed as  $\mathbf{v}_i^{\mathcal{O}_i} = [r_i w_i, k_{i,v} \sin k_{i,v} t]^T$  and  $w_i = k_{i,w}$ . Note that the control input first control stage is only to collect the historical measurement information and can be optimized according to the convergence speed or noise robustness and so on, we only give a feasible example. In the second control stage, the robot conducts formation control based on the estimation results of collaborative localization. The control input can be designed as  $\mathbf{v}_i^{\mathcal{O}_i} = \hat{\mathbf{v}}_i - \begin{bmatrix} k_2 & k_3 w_0 & 0 \\ 0 & 0 & k_4 \end{bmatrix} \hat{\epsilon}_{i,p}$  and  $w_i = \hat{w}_i - k_5 \hat{\epsilon}_{i,s}$ , where  $\hat{\mathbf{v}}_i$  and  $\hat{w}_i$  are designed to estimate the linear velocity and yaw rate of the leader robot. The update law of them are designed as  $\dot{\hat{\mathbf{v}}}_i = -k_1 e_{i,v} - \frac{e_{i,v}^T}{\sqrt{e_{i,v}^T e_{i,v} + \delta}} \hat{F}_{i,v}$  and  $\dot{\hat{w}}_i = -k_1 e_{i,w} - \frac{e_{i,w}}{\sqrt{e_{i,w}^2 + \delta}} \hat{F}_{i,w}$ , where  $e_{i,v}$  and  $e_{i,w}$  are designed as  $e_{i,v} = \sum_{j \in \mathcal{N}_i} a_{ij} (\hat{\mathbf{v}}_i - \hat{\mathbf{v}}_j) + \mu_i (\hat{\mathbf{v}}_i - \mathbf{v}_0^{\mathcal{O}_0})$  and  $e_{i,w} = \sum_{j \in \mathcal{N}_i} a_{ij} (\hat{w}_i - \hat{w}_j) + \mu_i (\hat{w}_i - w_0)$ . The update law of  $F_{i,v}$  and  $F_{i,w}$  are  $\dot{F}_{i,v} = \sum_{j \in \mathcal{N}_i} a_{ij} (\hat{F}_{i,v} - \hat{F}_{j,v}) + \mu_i (\hat{F}_{i,v} - F_v)$  and  $\dot{F}_{i,w} = \sum_{j \in \mathcal{N}_i} a_{ij} (\hat{F}_{i,w} - \hat{F}_{j,w}) + \mu_i (\hat{F}_{i,w} - F_w)$ , where  $F_v = a_{\max}$  and  $F_w = \alpha_{\max}$ . According to Theorem 3 in [15], the formation error  $\epsilon_i$  converges to  $\mathbf{0}$  asymptotically if and only if Assumption 2 is satisfied for each  $(i, j) \in \mathcal{G}$  and the yaw rate of the leader satisfies  $w_0 > 0$ .

### B. Experiment results

The distributed 3-D formation experiments are carried out in an indoor environment. A kind of micro-UAV Crazyflie with a dynamics model conforming to Eq.(11) is adopted as the experimental platform. The underlying control method of the platform can be found in the Appendix D. Each robot is equipped with an IO to measure its own translational displacement and rotational displacement. The relative measurement topology is shown in Fig.3(a) and the experimental scene is shown in Fig.3(b). Due to the limitation of the capability of

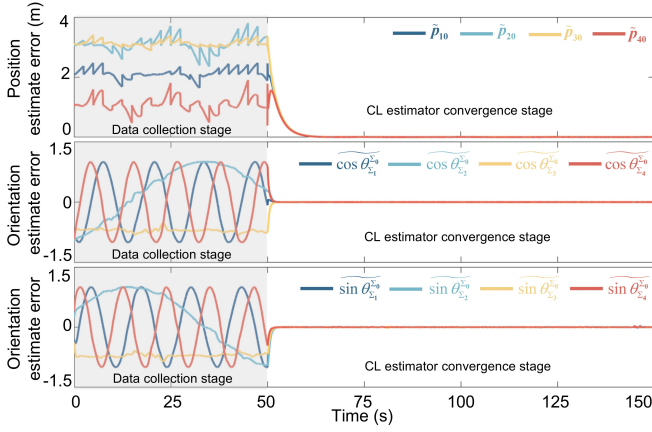


Fig. 4. Cooperative localization estimation error of each robot  $i$ .

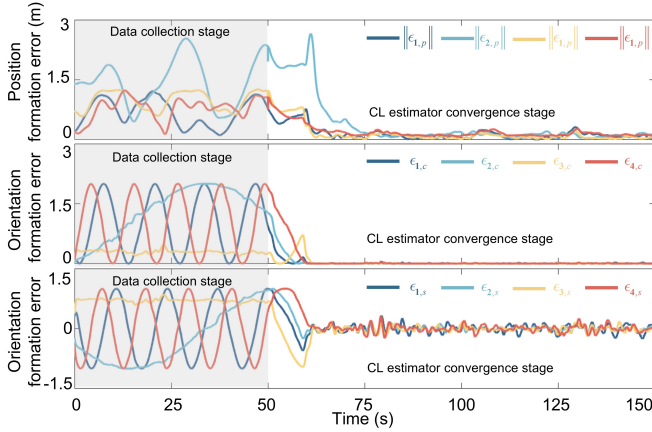


Fig. 5. Formation tracking error of each robot  $i$ .

the micro UAV to carry sensors, we used motion capture to measure the relative distance, orientation and position between the UAV and its neighbors in the odometer frame of each UAV, similar experimental strategy also appeared in relative localization result [18]. In practical applications, these signals can be measured by UWB, radar, camera or other sensors. [The analysis of noise measurement for CL estimation error can be found in Appendix C.](#) 5 threads running on a ground working station, each thread  $i$  receives the real-time measurement information of robot  $i$ . The proposed distributed CL strategy and control law are executed by thread  $i$ . Parameters used in the CL estimators are  $\Delta t = 0.02$ ,  $k_1 = 2$ ,  $\alpha = 0.05$ ,  $\beta = 2$ . Parameters adopted in the control method are  $v_{\max} = 1$  m/s,  $a_{\max} = 1\text{m/s}^2$ ,  $\alpha_{\max} = 0.2\text{rad/s}^2$ ,  $r_0 = r_3 = 0.3\text{m}$ ,  $r_1 = r_4 = 0.4\text{m}$ ,  $r_2 = 0.6\text{m}$ ,  $w_0 = w_3 = 0.4\text{rad/s}$ ,  $w_1 = -0.2\text{rad/s}$ ,  $w_2 = 0.3\text{rad/s}$ ,  $w_4 = -0.3\text{rad/s}$ ,  $k_{0,v} = 0.4$ ,  $k_{1,v} = 0.8$ ,  $k_{2,v} = -0.4$ ,  $k_{3,v} = -0.8$ ,  $k_{4,v} = 1.2$ .  $k_2 = 2$ ,  $k_3 = 7$ ,  $k_4 = 0.3$ ,  $k_2 = 1$ . In this experiment <sup>1</sup>, motion capture system is used to record the ground truth pose of the robots. The CL estimation error  $\tilde{p}_{i0}$ ,  $\cos \theta_{\Sigma_i}^{\Sigma_0}$  and  $\sin \theta_{\Sigma_i}^{\Sigma_0}$  are shown in Fig.(4). The formation control tracking error  $\|\epsilon_{i,p}\|$ ,  $\epsilon_{i,c}$  and  $\epsilon_{i,s}$  are shown in Fig.(5). One can see that when the measurement data is collected sufficiently, both the estimation error and tracking error fast converge.

<sup>1</sup>Experiment media available: <https://youtu.be/wQRBr9uJfmg>

TABLE I  
MAIN SYMBOLS USED IN THIS PAPER

Symbol	Description
$\mathcal{O}_i, \Sigma_i$	Odometry and Body frame of robot $i$ .
$T_{\mathcal{O}_j}^{\mathcal{O}_i}$	Initial relative pose between frames $\mathcal{O}_i$ and $\mathcal{O}_j$ .
$y_{ij}(t_k)$	Innovation constructed from relative measurements.
$\Phi_{ij}^{\mathcal{O}_i}(t_k)$	Regression basis vector for relative localization.
$\hat{p}_{i,t_0}, \hat{R}_{\mathcal{O}_i}^{\mathcal{O}_0}$	Estimate the initial relative pose between robots $i$ and the leader.
$\hat{z}_i, \hat{R}_{\Sigma_0}^{\mathcal{O}_0}$	Estimate of the leader's odometry information.
$\hat{p}_{i0}^{\Sigma_i}, \hat{R}_{\Sigma_i}^{\Sigma_0}$	Estimate the real-time relative pose between robots $i$ and the leader.

**Algorithm 1:** Distributed localization algorithm (RL-CL cascade)

```

1
  Input: Local odometry  $z_i^{\mathcal{O}_i}(t_k)$ ,  $R_{\Sigma_i}^{\mathcal{O}_i}(t_k)$ ; relative
    measurements  $m_{ij}^{\Sigma_i}(t_k)$ ; received neighbor odometry
     $z_j^{\mathcal{O}_j}(t_k)$ ,  $R_{\Sigma_j}^{\mathcal{O}_j}(t_k)$ .
  Output: RL estimates  $\hat{\Theta}_{ij}^*(t_k)$ ; CL estimates
     $\hat{p}_{i0}(t_k)$ ,  $\hat{R}_{\Sigma_i}^{\Sigma_0}(t_k)$ .

2 while each sampling instant  $t_k$  do
3   for each neighbor  $j \in \mathcal{N}_i$  do
4     Construct regression pair  $(y_{ij}(t_k), \Phi_{ij}^{\mathcal{O}_i}(t_k))$ ;
5     Update parameter estimator  $\hat{\Theta}_{ij}$  using Eq.(14);
6     Recover initial relative pose estimate  $\hat{\Theta}_{ij}^*$  using
       Eq.(15);
7   Update distributed coupled estimators  $\hat{p}_{i,t_0}, \hat{R}_{\mathcal{O}_i}^{\mathcal{O}_0}$  using
       Eq.(18);
8   Update distributed observers  $\hat{z}_i, \hat{R}_{\Sigma_0}^{\mathcal{O}_0}$  using Eq.(19);
9   Compute CL estimators  $\hat{p}_{i0}^{\Sigma_i}$  and  $\hat{R}_{\Sigma_i}^{\Sigma_0}$  using Eq.(17);

```

## VI. CONCLUSION

In this paper, we have proposed a unified CL algorithm for heterogeneous measurement swarm. With the proposed data-driven RL estimator, the RL task is achieved for each pair of neighboring robots in the measurement topology. The proposed pose coupling estimator realized the CL task of the swarm system under weakly connected measurement topology, which is also the least restrictive measurement topology condition in the existing results. The effectiveness of the proposed method is demonstrated through its application to the real-world formation control task of five nonholonomic UAVs.

## APPENDIX A

### NOTATION LIST OF THE PROPOSED METHOD

For ease of reading, in this section, we provide a table of the main symbols that appear in this article in the following Table I.

## APPENDIX B

### PSEUDOCODE OF THE PROPOSED METHOD

The pseudocode of the proposed data-driven localization method is shown in Algorithm 1. At each sampling instant,

the robot first performs relative localization (RL) with respect to its neighbors by constructing scalar regression pairs and updating the corresponding parameter estimator ( $\hat{\Theta}_{ij}^*$ ). The recovered initial relative pose estimates are then fused through a distributed coupled estimator ( $\hat{p}_{i,t_0}$ ,  $\hat{R}_{\Sigma_i}^{O_i}$ ) to estimate the robot's initial pose relative to the leader. In parallel, a distributed observer ( $\hat{z}_i$ ,  $\hat{R}_{\Sigma_0}^{O_0}$ ) is employed to estimate the leader's real-time odometric displacement and angular displacement. Finally, the cooperative localization (CL) estimate ( $\hat{p}_{i0}^{\Sigma_i}$  and  $\hat{R}_{\Sigma_i}^{\Sigma_0}$ ) of the robot's real-time pose with respect to the leader is obtained by combining the estimated initial relative pose and the observed leader motion.

### APPENDIX C

#### DISCUSSION ON THE MEASUREMENT NOISE

In reality, both relative sensors (such as UWB, camera) and odometer sensors have measurement errors, which is also a key concern for us in the repair process. But for most measurements, it can be considered that the measurement error is bounded. Even for some measurements with relatively large errors, they can be effectively eliminated based on some outlier detection algorithms [15]. Therefore, it is reasonable to assume that the measurement error is bounded, which is also mentioned in many related achievements. In our distributed localization framework, the overall design consists of two interconnected components. The first component is the relative localization (RL) between each agent and its neighbors, while the second component is a cooperative localization (CL) module, in which each agent estimates the relative pose of the leader by exploiting information exchanged with its neighbors. The observations involved in these two components are cascaded.

Next, we provide a detailed analysis of how the bounded sensor measurement noise propagates through the system and affects the final performance of cooperative localization. Specifically, we first analyze the impact of measurement noise on the relative localization stage. Based on this analysis, we then investigate how the noise influences the convergence properties of the cooperative localization error. When the sensor measurement error is bounded, the error of the innovation  $y_{ij}$  and the norm of basis function  $\Phi_{ij}$  is also bounded. Reference [19] analyzed the estimation error of parallel learning in the presence of measurement noise. According to its theorem 1 in [19], when the measurement error is bounded, there is a linear relationship between the estimation error and the upper bound of the error of the innovation  $y_{ij}$  and the norm of basis function  $\Phi_{ij}$ . As a result, under the bounded measurement error condition, one can see that for each robot  $i$  and its neighbor robot  $j$ , the RL error  $\tilde{p}_{ij,t_0}$ ,  $\tilde{c}_{i,t_0}(t)$  and  $\tilde{s}_{i,t_0}(t)$  are bounded.

Based on the above analysis, the boundedness of the RL errors further implies that the disturbance terms appearing in the cooperative localization error dynamics are bounded. For the position estimation part of CL, recall that the estimation error dynamics is given by

$$\dot{\tilde{p}}_{t_0} = -((\mathcal{L} + \mathcal{B}) \otimes \mathbf{I}_{3 \times 3}) \tilde{p}_{t_0} + \Xi_p, \quad (22)$$

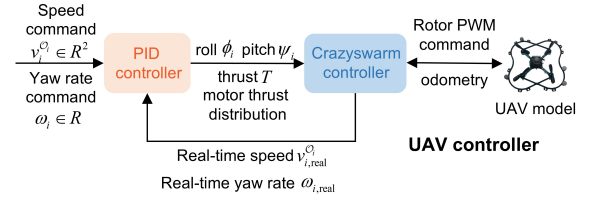


Fig. 6. UAV controller based on IMU and odometer.

where the disturbance term  $\Xi_p$  depends on the RL estimation errors. Since the RL errors  $\tilde{p}_{ij,t_0}$ ,  $\tilde{c}_{ij,t_0}$  and  $\tilde{s}_{ij,t_0}$  are bounded, it follows that  $\Xi_p$  is also bounded. Under Assumption 1 in the revised manuscript, the matrix  $(\mathcal{L} + \mathcal{B})$  is positive definite. Therefore, the position estimation error dynamics is input-to-state stable with respect to  $\Xi_p$ , which implies that  $\tilde{p}_{t_0}$  is uniformly ultimately bounded in the presence of bounded measurement noise. For the attitude estimation part, the cooperative localization error satisfies

$$\dot{\tilde{\chi}}_{t_0} \leq -(\mathcal{L}_{\tilde{R}} + \mathcal{B} \otimes \mathbf{I}_{2 \times 2}) \tilde{\chi}_{t_0} + \|\Xi_a\| \|\tilde{\chi}_{t_0}\| + \|\Xi_a\|, \quad (23)$$

where  $\Xi_a$  is constructed from the RL attitude estimation errors and is directly related to the measurement noise level. Under Assumption 1, the matrix  $\mathcal{L}_{\tilde{R}} + \mathcal{B} \otimes \mathbf{I}_{2 \times 2}$  is positive definite. Therefore, the attitude error dynamics can be interpreted as a stable linear system subject to bounded multiplicative and additive perturbations. When the noise level is not high, by employing standard Lyapunov analysis together with Young's inequality, the negative definite term associated with  $\mathcal{L}_{\tilde{R}} + \mathcal{B} \otimes \mathbf{I}_{2 \times 2}$  can dominate the coupling term  $\|\Xi_a\| \|\tilde{\chi}_{t_0}\|$ . As a result, the attitude estimation error  $\tilde{\chi}_{t_0}$  is uniformly ultimately bounded.

### APPENDIX D

#### EXPERIMENTAL PLATFORM

In the experimental validation, quadrotors are controlled in a manner consistent with model Eq.(11). As show in Fig. 6, the control interface of the aerial robot accepts the velocity command  $v_i^{O_i}$  and yaw rate command  $w_i$ . The quadrotor regulates its horizontal motion by adjusting pitch angle  $\psi_i$  and roll angle  $\phi_i$ , which are accurately measured by the IMU and controlled in closed loop by the underlying flight controller (e.g., CrazySwarm controller). The vertical velocity and yaw rate are regulated through thrust  $T$  and motor thrust distribution. Under this configuration, the quadrotors are consistent with the kinematic model adopted in the paper.

### REFERENCES

- [1] J. Lü, K. Ze, S. Yue, K. Liu, W. Wang, and G. Sun, "Concurrent-learning based relative localization in shape formation of robot swarms," *IEEE Trans. Autom. Sci. Eng.*, 2025.
- [2] X. Fang, L. Xie, and D. V. Dimarogonas, "Simultaneous distributed localization and formation tracking control via matrix-weighted position constraints," *Automatica*, vol. 175, p. 112188, 2025.
- [3] X. Fang, L. Xie, and X. Li, "Integrated relative-measurement-based network localization and formation maneuver control," *IEEE Trans. Autom. Control*, vol. 69, no. 3, pp. 1906–1913, 2023.
- [4] L. Chen, C. Liang, S. Yuan, M. Cao, and L. Xie, "Relative localizability and localization for multi-robot systems," *IEEE Trans. Robot.*, 2025.
- [5] S. Zhao and D. Zelazo, "Localizability and distributed protocols for bearing-based network localization in arbitrary dimensions," *Automatica*, vol. 69, pp. 334–341, 2016.

- [6] Y. Lv, Z. Wu, H. Zhang, Z. Wang, and H. Yan, "Local-bearing-based prescribed-time distributed localization of multiagent systems with noisy measurement," *IEEE Trans. Ind. Inform.*, 2024.
- [7] Q. Van Tran, B. D. Anderson, and H.-S. Ahn, "Pose localization of leader-follower networks with direction measurements," *Automatica*, vol. 120, p. 109125, 2020.
- [8] M. Boughellaba and A. Tayebi, "Bearing-based distributed pose estimation for multi-agent networks," *IEEE Control Syst. Lett.*, vol. 7, pp. 2617–2622, 2023.
- [9] C. Zheng, Y. Mi, H. Guo, H. Chen, Z. Lin, and S. Zhao, "Optimal spatial-temporal triangulation for bearing-only cooperative motion estimation," *Automatica*, vol. 175, p. 112216, 2025.
- [10] N. De Carli, E. Restrepo, and P. R. Giordano, "Adaptive observer from body-frame relative position measurements for cooperative localization," *IEEE Control Syst. Lett.*, 2024.
- [11] S. Wang, H. Wang, W. Che, and Q. Li, "Distributed leader-following formation control of networked mobile robots via global orientation estimation," *IEEE Trans. Netw. Sci. Eng.*, 2025.
- [12] Y. Liu and Z. Liu, "Distributed adaptive formation control of multi-agent systems with measurement noises," *Automatica*, vol. 150, p. 110857, 2023.
- [13] N. Biggs, *Algebraic graph theory*. Cambridge, U.K.: Cambridge university press, 1993.
- [14] J. Zhao, K. Zhu, H. Hu, X. Yu, X. Li, and H. Wang, "Formation control of networked mobile robots with unknown reference orientation," *IEEE-ASME Trans. Mechatron.*, vol. 28, no. 4, pp. 2200–2212, 2023.
- [15] K. Ze, W. Wang, S. Yue, G. Sun, K. Liu, and J. Lü, "Relative pose estimation for nonholonomic robot formation with uwb-io measurements," *arXiv preprint arXiv:2411.05481*, 2024.
- [16] X. Fang, X. Li, and L. Xie, "3-d distributed localization with mixed local relative measurements," *IEEE Trans. Signal Process.*, vol. 68, pp. 5869–5881, 2020.
- [17] K. Ze, W. Wang, K. Liu, and J. Lü, "Time-varying formation planning and distributed control for multiple uavs in clutter environment," *IEEE Trans. Ind. Electron.*, vol. 71, no. 9, pp. 11 305–11 315, 2023.
- [18] J. Li, Z. Ning, S. He, C.-H. Lee, and S. Zhao, "Three-dimensional bearing-only target following via observability-enhanced helical guidance," *IEEE Trans. Robot.*, vol. 39, no. 2, pp. 1509–1526, 2022.
- [19] M. Mühlegg, G. Chowdhary, and E. Johnson, "Concurrent learning adaptive control of linear systems with noisy measurements," in *AIAA Guidance, Navigation, and Control Conference*, 2012, p. 4669.